JGR Atmospheres

RESEARCH ARTICLE
10.1029/2021JD035567

A Post-Phaseout Retrospective Reassessment of the Global Methyl Bromide Budget

E. S. Saltzman[1], M. R. Nicewonger[2], S. A. Montzka[2], and S. A. Yvon-Lewis[3]

[1]Departments of Earth System Science and Chemistry, University of California, Irvine, CA, USA, [2]NOAA/GML National Oceanic and Atmospheric Administration, Boulder, CO, USA, [3]Department of Oceanography, Texas A&M University, College Station, TX, USA

Key Points:

- As a result of the Montreal Protocol phase-out, atmospheric methyl bromide declined over the past two decades and has recently stabilized
- The ocean saturation state for methyl bromide has increased and the oceans are a small net source to the atmosphere
- An imbalance between the known sources and losses of atmospheric methyl bromide remains, requiring additional emissions in the tropics

Supporting Information:

Supporting Information may be found in the online version of this article.

Correspondence to:

E. S. Saltzman,
esaltzma@uci.edu

Citation:

Saltzman, E. S., Nicewonger, M. R., Montzka, S. A., & Yvon-Lewis, S. A. (2022). A post-phaseout retrospective reassessment of the global methyl bromide budget. *Journal of Geophysical Research: Atmospheres*, *127*, e2021JD035567. https://doi.org/10.1029/2021JD035567

Received 21 JUL 2021
Accepted 15 JAN 2022

Author Contributions:

Conceptualization: E. S. Saltzman
Data curation: M. R. Nicewonger
Methodology: E. S. Saltzman, M. R. Nicewonger, S. A. Montzka, S. A. Yvon-Lewis
Software: E. S. Saltzman, M. R. Nicewonger
Visualization: M. R. Nicewonger
Writing – original draft: E. S. Saltzman
Writing – review & editing: E. S. Saltzman, M. R. Nicewonger, S. A. Montzka, S. A. Yvon-Lewis

Abstract Methyl bromide is a stratospheric ozone-depleting substance with both natural and anthropogenic sources. The global budget of methyl bromide has never been fully understood as evidenced by the significant budget gap between the bottom-up source estimates and calculated atmospheric losses. Atmospheric methyl bromide levels have declined significantly since Phase-out under the Montreal Protocol began in 1999, and the atmosphere appears to have reached a new steady state during the past five years. Here, we reassess the global methyl bromide budget utilizing the 25-year record of atmospheric methyl bromide measurements from the National Oceanic and Atmospheric Administration Global Monitoring Laboratory global flask network and a zonal 6-box coupled global ocean/atmosphere model. Model inversions were used to estimate the total emissions required to account for the observed atmospheric methyl bromide levels. From 1995 to 2019, global land-based emissions (natural and anthropogenic) declined from about 120 to 85 Gg y^{-1} and net ocean emissions increased from −5 to +5 Gg y^{-1}. There remains an imbalance between the bottom-up estimates of terrestrial sources and the inversion result. Based on the timing, magnitude, and spatial distribution of the imbalance we partition it into (a) a persistent or time invariant source located primarily in the tropics, and (b) a smaller time-varying component that scales with the anthropogenic source during phase-out. We hypothesize that the persistent source is likely natural and the time variant component is an artifact resulting from a slight underestimation of anthropogenic emissions.

Plain Language Summary Methyl bromide is an ozone-depleting gas for which production is globally controlled under the fully amended and adjusted Montreal Protocol. As a result, atmospheric methyl bromide levels have declined dramatically since 1999 as measured by the National Oceanic and Atmospheric Administration Global Monitoring Laboratory flask air network. The change in atmospheric methyl bromide abundance provides an opportunity to re-examine our understanding of the global budget. We use a coupled ocean/atmosphere model to estimate the change in emissions required to explain the observed atmospheric changes. The study suggests that anthropogenic emissions may have previously been slightly underestimated and that there remain significant sources of unknown origin, located mainly in the tropics.

1. Introduction

Methyl bromide is a halogenated trace gas emitted by both natural and anthropogenic sources. It is present in the troposphere at a global mean mole fraction of 6.6 ppt (2019 global mean; parts per trillion or pmol mol^{-1}) and has an atmospheric lifetime estimated at 0.8 years (Engel & Rigby, 2018). The atmospheric transport of methyl bromide to the stratosphere and the subsequent photochemical destruction contributes to the catalytic loss of stratospheric ozone. Methyl bromide is considered an ozone depleting substance and a multiyear phase-out was initiated in 1999 under the Copenhagen Amendments and subsequent Adjustments to the Montreal Protocol. Global industrial production of methyl bromide declined from over 70 Gg y^{-1} in 1995 to roughly 10 Gg y^{-1} in 2018 (UNEP, 2019). Some critical use exemptions and quarantine pre-shipment (QPS) uses for methyl bromide remain in effect today and account for this continued production (UNEP, 2014).

The major sources of atmospheric methyl bromide are biomass and biofuel burning, oceanic emissions, fumigation, and vegetation (Butler & Rodriguez, 1996; Deventer et al., 2018; Hardacre and Heal, 2013; Jiao et al., 2020; Lee-Taylor et al., 1998; Montzka et al., 2003; Rhew et al., 2010; Yvon-Lewis & Butler, 2002, 1996; Yvon-Lewis et at., 2009). The main sink of methyl bromide is via hydroxyl radical with a partial lifetime of 1.8 years (Engel & Rigby, 2018). Other sinks occur via soils, the ocean, and loss to the stratospheric with partial lifetimes of roughly

3.4 years, 2.7 years, and 26.3 years, respectively (Hu et al., 2012; Montzka & Reimann, 2011; Orkin et al., 2013; Yvon-Lewis & Butler, 1997). Numerous studies noted an imbalance between the known sources and estimated losses of methyl bromide from the atmosphere (Butler & Rodriguez, 1996; Lee-Taylor et al., 1998; Montzka et al., 2003; Yvon-Lewis & Butler, 1996, 2002; Yvon-Lewis et al., 2009). Using best estimates of sources and sinks for the late 1990s, more than 30 Gg of unknown sources were required in order to balance the global budget (Yvon-Lewis et al., 2009). The methyl bromide levels in preindustrial Antarctic ice cores show a similar budget gap, assuming that the natural components of the preindustrial budget (sources and sinks) were similar to the present day (Saltzman et al., 2004). It has generally been assumed that the budget gap is due to unaccounted for biogenic terrestrial emissions, but sources of sufficient magnitude have never been identified. This budget gap has been referred to in the literature as a "missing source" (Lee-Taylor et al., 1998; Yvon-Lewis et al., 2009).

The phase-out of anthropogenic production of methyl bromide and the subsequent atmospheric response constitutes a remarkable natural experiment that can be used to improve our understanding of the global budget and atmospheric lifetime of methyl bromide. As anthropogenic emissions were reduced, atmospheric methyl bromide mole fraction has declined and gradually approached a new steady state. Yvon-Lewis et al. (2009) showed that the decline in atmospheric methyl bromide from 1999 to 2005 was likely influenced by a perturbation in biomass burning emissions due to the 1997/1998 strong El Niño but was otherwise consistent with the prescribed phase-out. Hu et al. (2012) updated this analysis, extending the analysis from 1995 to 2010, and showed the atmospheric abundance would reach steady state around 2013 barring further reductions in anthropogenic emissions.

The oceans play a complex role in the global biogeochemical cycle of methyl bromide, with both production and destruction occurring in the surface oceans. As a result, the oceans can act as both a source and sink of methyl bromide to/from the atmosphere (Butler, 1994; Yvon-Lewis & Butler, 1996). Models predicted that the oceans would shift from a net sink during the 1990s to a net source after phase-out and this was confirmed by subsequent shipboard measurements (Hu et al., 2012; Yvon-Lewis et al., 2009). These changes in ocean saturation state present an opportunity to better assess the budget uncertainties in methyl bromide global models. This opportunity arises because as the saturation state of the oceans approached zero, ocean/atmosphere fluxes became negligible and the global budget became insensitive to the large uncertainties associated with parameterizations of air/sea gas exchange.

In this study, we examine the global biogeochemical cycle of methyl bromide using a 25-year record of atmospheric methyl bromide from the National Oceanic and Atmospheric Adminstration Global Monitoring Laboratory (NOAA GML) flask air network and an updated global model of atmosphere/ocean cycling. Implications for the magnitude and spatial/temporal variability of the methyl bromide budget gap between estimated sources and losses are discussed.

2. The NOAA GML Global Flask Air Data Set

The Halocarbons and other Atmospheric Trace Species Division of NOAA's Global Monitoring Laboratory (GML) has measured atmospheric methyl bromide at several sites across the globe for the past 25 years. Whole air samples from each site are obtained on average two to four times each month and analyzed by GC/MS at the Boulder, Colorado laboratory (Montzka et al., 2003). These data are updated regularly and available online (ftp://aftp.cmdl.noaa.gov/data/hats/methylhalides/ch3br/flasks). For this study, the data from each site were averaged to generate monthly mean methyl bromide abundances. These monthly means were averaged in 30° latitude zonal bands corresponding to the tropospheric model boxes described below.

Atmospheric samples are pressurized simultaneously in duplicate pairs of flasks. At most sites, the air is collected primarily in stainless steel flasks. Samples from South Pole and Summit, Greenland are stored in glass flasks because methyl bromide degrades in dry stainless steel flasks (Montzka et al., 2003). Several other sites include samples collected in glass (Palmer Station, Antarctica) or a combination of glass and stainless steel flasks (Cape Grim, Australia and South Pole). Flask pairs with relative differences above a threshold are excluded from the monthly mean calculation (roughly 12% of all flask pair measurements). The threshold has declined from 4% to 1.5% from 1995 to 2018 to reflect improvements in analytical precision over time. Flasks pairs with methyl bromide concentrations significantly higher or lower than expected for given times of year are also subjectively excluded from the monthly mean calculation.

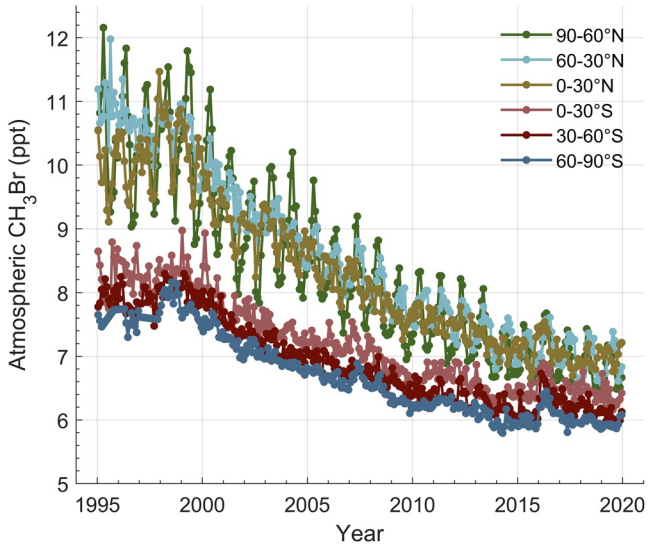

Figure 1. Monthly mean atmospheric methyl bromide levels averaged into 30° latitude zonal bands from 1995 to 2019 measured by the National Oceanographic and Atmospheric Administration Global Monitoring Laboratory global flask air network.

The methyl bromide standard scale is developed at NOAA GML using gravimetric and static dilution techniques (Montzka et al., 2003). The scale is based on parts per million-level standards made in 1995, 2001, and 2002. More information about the methyl bromide standard can be found at: https://www.esrl.noaa.gov/gmd/ccl/scales/CH3Br_tree.jpg. The stability of the calibration scale over time is assessed with archived air stored in high pressure stainless-steel (humid air) and aluminum (dry air) cylinders.

The monthly mean latitudinal methyl bromide mixing ratios (Figure 1) were calculated by averaging monthly mean methyl bromide from sites located in the the same 30° bin. Three sites were used for the 90°–60°N bin: Alert, Canada, Summit, Greenland, and Utqiagvik (Barrow), Alaska. Five sites were used for the 60°–30°N bin: Mace Head, Ireland, Park Falls, Wisconsin, Harvard Forest, Massachussetts, Trinidad Head, California, and Niwot Ridge, Colorado. Two sites were used for the 0°–30°N bin: Cape Kumakahi and Mauna Loa, Hawaii. One site was used for the 0°–30°S bin: Samoa, American Samoa. Two sites were used for the 30–60°S bin: Cape Grim, Australia, and Palmer Station, Antarctica. One site was used for the 60°–90°S bin: South Pole, Antarctica. More details about each specific site is found at: https://www.esrl.noaa.gov/gmd/hats/flask/flasks.html. For a given site, missing observations were filled in with linear interpolation between nearest months. The standard deviation of the monthly mean methyl bromide value for each latitudinal bin was calculated by taking the square root of the sum of the individual site's monthly standard deviation squared. Monthly standard deviations are generally larger earlier in the record (i.e., 1995–2000) in part because of larger atmospheric gradients during those years, and because of subsequent improvements in measurement precision. For the full length of the record (1995–2019), the average monthy standard deviation for the latitudinal bins from north to south are 0.43, 0.68, 0.31, 0.21, 0.19, and 0.31 ppt, respectively.

3. Model

The modeling strategy employed in this study is to develop a global biogeochemical model of methyl bromide with an explicit parameterization of oceanic cycling and ocean/atmosphere exchange. The model is run in the following modes:

1. Inverse mode–In inverse mode, terrestrial methyl bromide sources are calculated to optimize a weighted least squares deviation between the atmospheric abundance of methyl bromide in the model and the NOAA GML network flask measurements at monthly time resolution. The optimized terrestrial emissions are compared to estimates of the known natural and anthropogenic sources in order to assess the magnitude and spatial/temporal variations of the “budget gap” or “missing source” identified in many prior studies.
2. Forward mode–In forward mode, terrestrial emissions are specified and the atmospheric abundance of methyl bromide is calculated on a monthly basis for a specified number of years. Forward model runs can utilize the optimized terrestrial emissions from an inverse run or other emission scenarios.

3.1. Model Description

The model computes the mass balance for tropospheric methyl bromide incorporating terrestrial emissions (natural and anthropogenic), ocean/atmosphere invasion and evasion, and atmospheric losses to photochemistry, soils, vegetation, and stratospheric transport (Table S1 in Supporting Information S1). The atmosphere is represented with six zonal tropospheric boxes, each 30° wide in latitude. Transport between the boxes is parameterized by seasonally varying exchange coefficients based on the global budget of SF_6 (Marik, 1998; Mitchell et al., 2013). Transport is specified to be the same for all years.

The surface ocean is represented in the model as a 2 × 2° grid of cells with prescribed monthly mixed layer depth, sea surface temperature, wind speed, and salinity based on climatological and satellite-derived products given in Table S1 in Supporting Information S1. Oceanic losses include chemical degradation, mixing through

the thermocline, and evasion to the atmosphere (Butler, 1994: Yvon-Lewis & Butler, 1996, 1997). Oceanic inputs are biological production and atmospheric input (invasion). Biological production is set at 1999 levels based on King et al. (2002) with coastal production rates from Hu et al. (2012). Each ocean box exchanges methyl bromide with the overlying atmosphere with no lateral ocean transport. Earlier methyl bromide modeling studies were conducted with a similar ocean model using a 1 × 1° grid and a two box troposphere (N and S hemispheres; Saltzman et al., 2004; Yvon-Lewis & Butler, 2002; Yvon-Lewis et al., 2009). The current model is coded in MATLAB (Mathworks, Inc.). The model is integrated using the MATLAB ODE45 variable time step ODE solver and inversions were carried out using MATLAB *fmincon* function. All inputs used in the model calculation are specified as monthly average values.

Model inversions were carried out to determine the total terrestrial emissions required to achieve optimal agreement between the model and the NOAA GML atmospheric methyl bromide data. The MATLAB function *fmincon* was used to optimize the monthly emissions in each box by minimizing the following cost function:

$$\text{cost} = \frac{1}{\text{mass}_{\text{trop}}} \sum_{\text{box}} \sum_{\text{month}} w * \text{mass}_{\text{box}} (Y_{\text{box}} - Y_{\text{NOAA}})^2 \quad (1)$$

where Y_{box} and Y_{NOAA} are the modeled and observed monthly mixing ratios of methyl bromide in each 30° wide zonal model tropospheric box and w is a weighting factor for the six atmospheric boxes (weight = [1 4 4 4 4 1]). The model inversion was carried out on overlapping 2 year segments in which the atmosphere is initialized by atmospheric observations, and the cost function is calculated based on a 2 year model run. Only the second year's optimized results are used. The starting time is then incremented by 1 year and the process is repeated. This inversion process results in a 25 year record of optimized emissions in each model box. Those emissions are used in a forward mode run to compute the final time series, which reproduces the monthly atmospheric observations to within 3% across all years and boxes. This procedure was computationally much more efficient than attempting to simultaneously optimize the entire 25 years record.

3.2. Methyl Bromide Atmospheric Losses in the Model

Atmospheric losses in the model are scaled to achieve e-folding lifetimes consistent with the literature. Photochemical losses are defined by monthly OH and temperature fields from Spivakovsky et al. (2000) and the temperature-dependent rate constant from Burkholder et al. (2015). The OH fields are scaled by a factor of 0.72 to give a global photochemical methane lifetime of 10.4 years (Prather et al., 2012). This yields a tropospheric methyl bromide lifetime with respect to OH oxidation of 1.8 years. The loss of atmospheric methyl bromide to soils is scaled to a tropospheric lifetime of 3.4 years (Montzka & Reimann, 2011) with a spatial/temporal distribution scaled to the ISLSCP II MODIS land cover product (Friedl et al., 2010) and seasonality from Shorter et al. (1995) with no interannual variability. Loss to the stratosphere is scaled to give a constant partial tropospheric lifetime of 26.3 years (Orkin et al., 2013). The oceans are both a source and sink for methyl bromide in the model, as discussed in Section 3.3.

3.3. Oceanic Cycling and Air/Sea Exchange of Methyl Bromide

Methyl bromide in each 2 × 2°ocean cell is computed dynamically from the mass balance of production and loss. The approach and terminology used here are based on Yvon-Lewis & Butler (1996, 2002). The mass of methyl bromide in each ocean cell reflects a balance between the sources (biological production and atmospheric input) and the losses (hydrolysis, chloride substitution, biological degradation, downward mixing through the thermocline, and loss to the atmosphere). Oceanic losses consist of chemical loss via hydrolysis and chloride substitution, biological uptake, vertical mixing through the thermocline, and loss to the atmosphere (see Table S1 in Supporting Information S1).

There are no direct measurements of biological production of methyl bromide in the oceans. Instead, the rate of biological production in each ocean cell is calculated in order to achieve agreement with the observed sea surface saturation state during the 1990s using the saturation versus sea surface temperature relationship developed by King et al. (2002) and described in Saltzman et al. (2004). Production rates for coastal waters (<200 m depth) were modified as recommended by Hu et al. (2012) using seafloor topography from Smith and Sandwell (1997).

Air/sea gas fluxes are computed in the model as follows:

$$F_{\text{evasion}} = k_{\text{gas}} * C_{\text{seawater}} \quad (2)$$

$$F_{\text{invasion}} = - \ k_{\text{gas}} * p_{\text{atm}} * H \quad (3)$$

$$F_{\text{net}} = F_{\text{evasion}} - F_{\text{invasion}} \quad (4)$$

where F_{evasion} and F_{invasion} are the fluxes of methyl bromide out of and into the ocean (moles m^{-2} day^{-1}), C_{seawater} is the concentration of methyl bromide in surface seawater (moles m^{-3}), H is the solubility of methyl bromide in seawater at a given temperature and salinity (mol m^{-3} atm^{-1}; De Bruyn & Saltzman, 1997b), ρ_{atm} is the partial pressure of methyl bromide over the sea surface, and k_{gas} is the gas transfer coefficient (m day^{-1}) expressed in water-side units.

Temperature-dependent properties and processes for the ocean model were calculated using monthly mean sea surface temperatures from the NOAA Optimum Interpolation (V2; Reynolds et al., 2002). Cross Calibrated Multi-Platform ocean surface winds (CCMP; 0.25 × 0.25°, 6 hourly) were used either as monthly means of $<U>$ or $<U^2>$ in the gas transfer parameterizations described below (Wentz et al., 2015).

Three parameterizations for the gas transfer coefficient (k_{gas}) were used in this study in order to capture the uncertainty associated with ocean/atmosphere exchange. These are:

W14–The Wanninkhof (2014) parameterization is derived from the long-term average gas transfer of $^{14}CO_2$ estimated from natural ^{14}C disequilibrium and the ocean inventory of bomb ^{14}C using an inverse global ocean modeling approach (Atlas et al., 2011; Naegler & Levin, 2006; Naegler, 2009; Sweeney et al., 2007). This parameterization assumes a quadratic dependence of gas transfer coefficient on wind speed and was developed using CCMP winds and an updated inventory of ^{14}C in the oceans (Wentz et al., 2015). The W14 parameterization is as follows:

$$k_{\text{gas\_W14}} = 0.251 * < U^2 > * (\text{Sc}_{\text{gas}}/660)^{-0.5} \quad (5)$$

Sc_{gas} is the temperature-dependent Schmidt number of methyl bromide (De Bruyn & Saltzman, 1997b; Table S1 in Supporting Information S1) and $<U^2>$ is the monthly mean of the squared 6-hourly winds. This parameterization does not discriminate between gas transfer by turbulent and bubble-mediated mechanisms. Consequently, methyl bromide solubility does not influence the gas transfer coefficient.

N00–The Nightingale et al. (2000) parameterization is a second order regression to deliberate dual tracer (^3He/SF_6) experiments conducted at sea:

$$k_{\text{gas\_N00}} = (0.333 * < U > + \ 0.222 * < U >^2) * (\text{Sc}_{\text{gas}}/660)^{-0.5} \quad (6)$$

The N00 parameterization gives good agreement with all dual tracer experiments to date (Ho et al., 2011). Like W14, this parameterization does not distinguish between turbulent and bubble-mediated mechanisms and is insensitive to trace gas solubility.

COAREG 3.6–Fairall et al. (2000, 2011) developed this physically based gas transfer model coupled to the NOAA COARE micrometeorological model for sensible heat, latent heat, and momentum fluxes. The gas transfer coefficient is parameterized as the inverse of the sum of water side and air side resistance, as follows:

$$k = \frac{u_*}{r_{\text{water}} + \alpha * r_{\text{air}}} \quad (7)$$

where u_* is friction velocity and α is dimensionless solubility. The water side resistance (r_{water}) in COAREG is separated into two components, turbulent/molecular diffusion (denoted as r_t) and bubble-mediated transfer (denoted as r_b or $1/k_b$) and the overall transfer velocity becomes:

$$k = \left[\frac{u_*}{r_{\text{water\_turbulent}}} + k_b\right]\left[\frac{1}{1 + \alpha * r_{\text{air}}/r_{\text{water}}}\right] \quad (8)$$

The model describes turbulent/molecular resistance using a "law of the wall" approach, with diffusion dominating transport near the interface, and surface wind stress driving mixing on both sides of the air/sea interface.

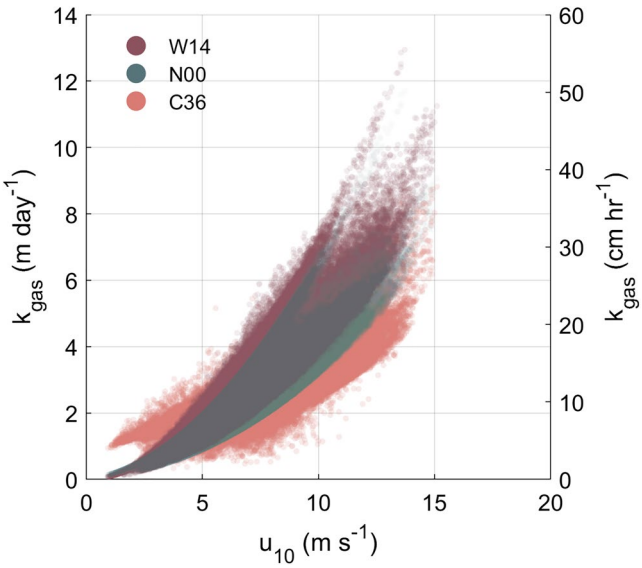

Figure 2. Gas transfer coefficients (k_{gas}) for methyl bromide as a function of wind speed, computed using the 2 × 2° ocean model, Cross Calibrated Multi-Platform winds and the following parameterizations: W14 (Wanninkhof, 2014), N00 (Nightingale et al., 2000); COAREG 3.6 (Fairall et al., 2011). k_{gas} is given at in situ temperatures for all ocean cells for the year 1990.

The turbulent resistance is scaled by $Sc^{-0.5}$ A separate term represents the transfer due to the equilibration of bubbles generated from wave breaking (Woolf, 1997). Gas solubility (α) influences both (a) the relative magnitude of air side and water side resistance, and (b) bubble transfer. Friction velocity is partitioned into two components, a tangential component (u_{*t}) and a wave component (u_{*g}), used to scale the turbulent/molecular and bubble terms, respectively. In this study, tunable constants of A = 1.6, B = 1.8 were used with the Woolf parameterization for bubble transfer. The explicit inclusion of bubble-mediated gas transfer in COAREG3.6 means that gas transfer coefficients are influenced by seawater temperature through its influence on both Schmidt number (as $Sc^{-0.5}$) and gas solubility.

Note that although the methyl bromide model runs with a 2 × 2° ocean grid, the gas transfer parameterizations are nonlinear and sensitive to the wind speed variance. The gas transfer coefficients were computed using the full resolution grid (0.25 × 0.25°, 6 hourly) CCMP wind fields and averaged to create the 2 × 2° grid.

There are significant differences between the various gas transfer parameterizations in terms of both magnitude and wind speed-dependence (Figure 2). W14 and N00 are quadratic functions of wind speed, leading to very strong (nonphysical) gas transfer rates at very high wind speeds. Both are also forced to zero gas transfer at zero winds, while COAREG3.6 allows some gas transfer due to buoyancy and gustiness. All of the parameterizations are relatively similar at moderate winds. The global area-weighted mean for three parameterizations ranges by roughly 20%. For example, the 1990 area-weighted mean k_{gas} values are 2.72, 3.38, and 3.04 m d^{-1} for COAREG 3.6, W14, and N00.

The Sc numbers of methyl bromide and CO_2 in seawater are nearly identical (Figure 3). However, the solubility of methyl bromide in seawater is about five fold greater than that of CO_2 (Figure 3; De Bruyn & Saltzman, 1997b; Wanninkhof, 1992). This affects two aspects of gas transfer: (a) the relative importance of water side and air side resistance, and (b) bubble-mediated gas transfer. Air side resistance is small for methyl bromide, comprising less than 5% of the total resistance even at low temperatures. This is illustrated using the air gradient fraction as defined by McGillis et al. (2000):

$$\gamma = \frac{1}{\left(1 + \frac{r_{water}}{\alpha * r_{air}}\right)} \tag{9}$$

where α is dimensionless solubility and r is the resistance to gas transfer on the air and water side, respectively.

Bubble-mediated gas transfer scales exponentially with wind speed and linearly with solubility. Consequently, at high wind speeds Sc-corrected tracer-based parameterizations likely overestimate the gas transfer coefficient for methyl bromide. The physically based COAREG3.6 parameterization partitions gas transfer between turbulent and bubble–mediated exchange and therefore explicitly takes solubility into account. As a result, gas transfer velocities are lower at high winds for methyl bromide than they would for a less soluble gas like CO_2. Figure 4 shows the relative contributions of turbulent/molecular and bubble-mediated processes to the total air/sea gas transfer velocity of CH_3Br. Uncertainties in modeling bubble generation and bubble distributions remains a major uncertainty in gas transfer and a subject of active research (Wanninkhof et al., 2009).

The net ocean/atmosphere exchange of methyl bromide is computed as the sum of invasion (from atmosphere to ocean) and evasion (from ocean to atmosphere; Yvon-Lewis & Butler, 1997). Invasion refers to the air/sea flux into each ocean cell computed as if the ocean concentration of methyl bromide was zero, and integrated globally, as follows:

$$\text{invasion} = \sum_{\text{ocean cells}} H * k_{gas} * x_{mebr} * \rho_{air} * m_w * A_{cell} \tag{10}$$

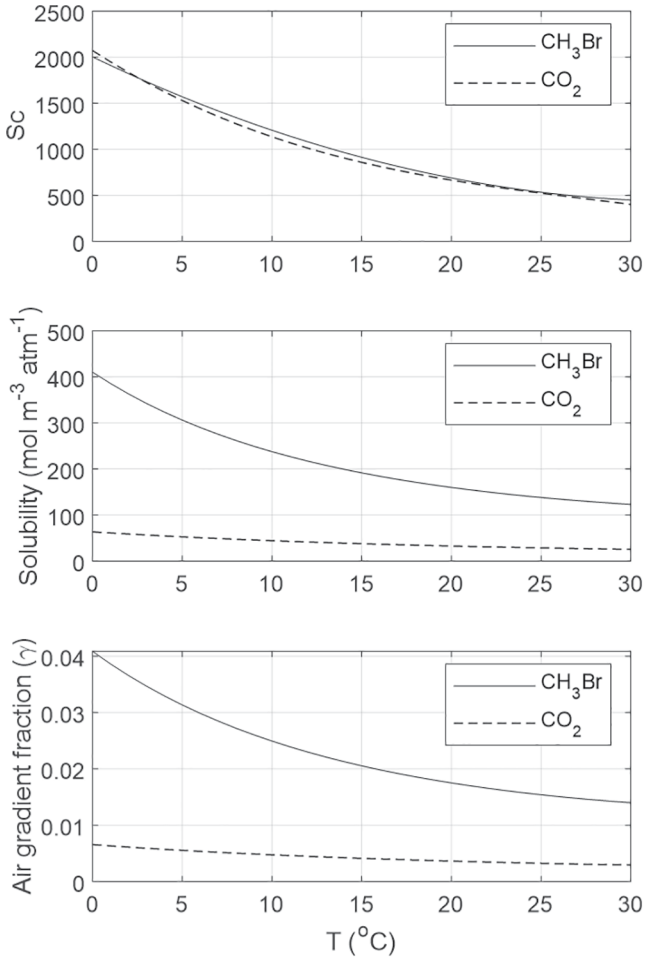

Figure 3. Physical properties of CH_3Br and CO_2 relevant to gas transfer shown as a function of temperature at a salinity of 35‰. From top: 1) Schmidt (Sc)-number in seawater, 2) seawater solubility, and 3) air gradient fraction (McGillis et al., 2000), defined as the fraction of air/sea concentration difference on the atmospheric side of the interface, computed using COAREG 3.6. Sc and solubility data from De Bruyn & Saltzman (1997a,b) and Wanninkhof (1992).

where invasion (given here in mol y^{-1} but referred to elsewhere in Gg y^{-1}), H is solubility (mol m^{-3} atm^{-1}), k_{gas} is the gas transfer coefficient (m yr^{-1}), x_{mebr} is the mixing ratio (mole fraction) of methyl bromide in air, ρ is the density of surface air (atm), m_w is molecular weight, and A_{cell} is the surface area of each ocean cell (m^2).

Evasion is the sea to air transfer computed as if the atmospheric abundance of methyl bromide was zero, computed as follows:

$$\text{evasion} = \sum_{\text{ocean cells}} k_{gas} * C_{mebr\_sw} * A_{cell} \tag{11}$$

where evasion (given here in mol y^{-1}, but referred to elsewhere in Gg y^{-1}), C_{mebr_sw} is the concentration of methyl bromide in seawater (mol m^{-3}), and k_{gas} and A_{cell} are as above. The concentration of methyl bromide in the surface ocean is a function of biological production, chemical and biological loss, and gas transfer. The fraction of methyl bromide destroyed in the water column is a useful parameter to assess the importance of internal oceanic cycling relative to air/sea gas transfer. This fraction was defined as follows by Butler (1994):

$$R_o = \frac{k_o}{k_o + k_1} = \frac{k_o}{k_o + k_{gas}/z} \tag{12}$$

where k_o is the sum of the first order rate constants for chemical loss, biological loss, and downward mixing, and k_1 is the first order rate constant for gas exchange (k_{gas}/z, where z is mixed layer depth). At the limiting condition of $R_o = 1$, essentially all of the methyl bromide (derived from either biological production or air/sea exchange) is destroyed in the ocean. In that case, the oceanic concentration of methyl bromide (C_{mebr_sw}) would be insensitive to changes in atmospheric levels induced by external factors such as terrestrial emissions. By contrast, $R_o << 1$ means that C_{mebr_sw} would be strongly influenced by changes in atmospheric methyl bromide levels.

4. Results and Discussion

The methyl bromide global model inversion was carried out using each of the three air/sea gas transfer parameterizations (W14, N00, and COAREG 3.6). For each gas transfer parameterization, oceanic production of methyl bromide is adjusted to achieve agreement with ocean saturation anomalies during the late 1990s (King et al., 2002). Ocean evasion and invasion are determined dynamically. The model inversions yield estimates of total terrestrial emissions (sum of anthropogenic + natural) required to optimize agreement with observed atmospheric methyl bromide levels from the NOAA GML network. No *a priori* assumptions are made about the origin (natural vs. anthropogenic), seasonality, or latitudinal distributions of the emissions.

Model results are discussed in the following order:

1. Model simulations using different gas transfer parameterization are compared for four years, spanning the 25-year record (Figure 5). Here we assess the sensitivity of the methyl bromide budget to gas transfer parameterization and compare the results of this model to prior published models.
2. The full 25-year model inversion is discussed in detail using one of the three gas transfer parameterizations (COAREG 3.6; Figures 5 and 6). Results from the other two parameterizations (N00 and W14) are shown in Figures S1 and S2 in Supporting Information S1). The history of terrestrial emissions is estimated from the model inversion and compared to bottom-up emissions estimates. The budget gap between bottom-up emissions and emissions is examined and various modifications to the emissions are proposed to minimize the gap and understand its origin.

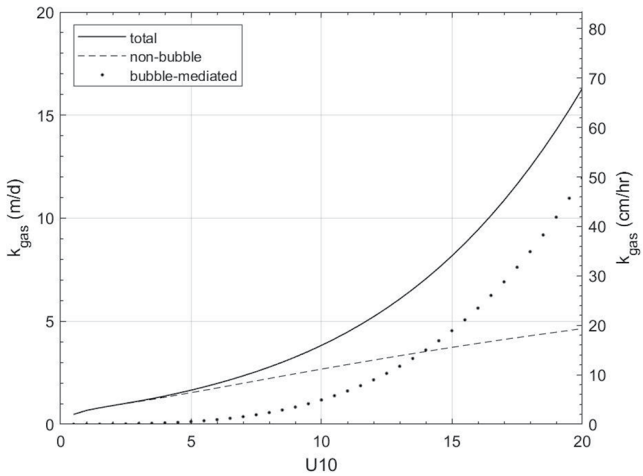

Figure 4. Relative contributions of turbulent/molecular and bubble-mediated processes to the total air/sea gas transfer velocity of CH_3Br. Calculated for 20°C and 35‰ salinity using COAREG 3.6.

3. A forward model run is presented to simulate a possible future emissions scenario with zero anthropogenic emissions of methyl bromide.

4.1. Influence of Gas Transfer Parameterization on the Methyl Bromide Budget

Model results using the three different gas transfer parameterizations gave broadly similar results with some subtle differences. To illustrate the differences, we extracted budget data from four periods (1995, 2005, 2010, and 2018; Figure 5; Table S2 in Supporting Information S1). The four time periods selected are:

Pre phase-out (1995)—This case represents the atmosphere just prior to initiation of methyl bromide phase-out under the Montreal Protocol and its Amendments. This represents the period of maximum anthropogenic emissions. Conditions for 1995 were used for comparison with Yvon-Lewis et al. (2009). Because of the high anthropogenic emissions, the atmospheric burden and total sources are the largest of the four simulations. Under this condition, the oceans are undersaturated and there is a large net flux of methyl bromide from the atmosphere into the ocean.

Mid phase-out (2005)—This case represents conditions six years after phase-out began. Based on the UNEP inventory data, anthropogenic production of methyl bromide had declined to about 40% below of pre phase-out production (UNEP, 2019). The atmospheric burden and total sources are reduced by more than 50% relative to pre phase-out conditions. This is a particularly interesting control case because the oceans were near equilibrium with respect to the atmosphere and the net air/sea flux is near zero. As a result, the global budget is relatively insensitive to gas transfer parameterization.

Late phase-out (2010)—This case is several years farther into phase-out. At this point, the oceans have become supersaturated in methyl bromide with respect to the atmosphere.

Modern (2018)—This case represents the near modern case where atmospheric methyl bromide levels have nearly stabilized at post phase-out levels. Some anthropogenic usage continues, but at much lower levels than prior to phase-out. The total sources in this case are the smallest of the four cases because of the continued decline in anthropogenic emissions. The oceans remain supersaturated, and the net air/sea flux is from the ocean to atmosphere.

The inversions including three gas transfer parameterizations yield a decrease in total terrestrial emissions (called "optimized emissions") from roughly 120 to 80 Gg y^{-1} between pre- and post phase-out periods (Figure 5). The sensitivity to gas transfer parameterizations is highest in the pre phase-out period (1995) when atmospheric methyl bromide levels were large and the oceans were a strong net sink. For example, net ocean exchange (emissions–uptake) for this period using the W14 and N00 parameterizations are −6.5 and −7.2 Gg y^{-1}, respectively. COAREG3.6 yields a smaller net ocean exchange of −4.6 Gg y^{-1}. This makes sense because ocean exchange scales roughly linearly with the gas transfer coefficient and the COAREG3.6 gas transfer coefficients are slightly smaller than those of the other two parameterizations. By 2005, the net ocean gas exchange is close to zero (−1.4 to 1 Gg y^{-1} for the various gas transfer parameterizations) because the surface ocean is near equilibrium with the troposphere. The net ocean gas exchange continues to increase after 2005, reaching 4–6 Gg y^{-1} in 2018.

As in previous studies, the known sources of methyl bromide are insufficient to balance the estimated losses. The budget gap is quantified by subtracting a bottom-up estimate of terrestrial emissions from the optimized terrestrial emissions required by each model inversion result. The four model inversions exhibit budget gaps ranging from 20 to 23 Gg y^{-1} in 1995 to about 15–17 Gg y^{-1} in 2018.

The gas transfer coefficient also has a significant effect on how the modeled saturation state of the ocean evolves during phase-out. The fraction R_o of methyl bromide lost in the water column due to hydrolysis, biological destruction, downward mixing, is useful in diagnosing this effect (Equation 12; Figure S3 in Supporting Information S1; Butler, 1994). In the limiting case of R_o approaching zero (rapid gas transfer, slow oceanic destruction), all methyl bromide produced or entering the ocean is emitted to the atmosphere. For R_o approaching unity (slow

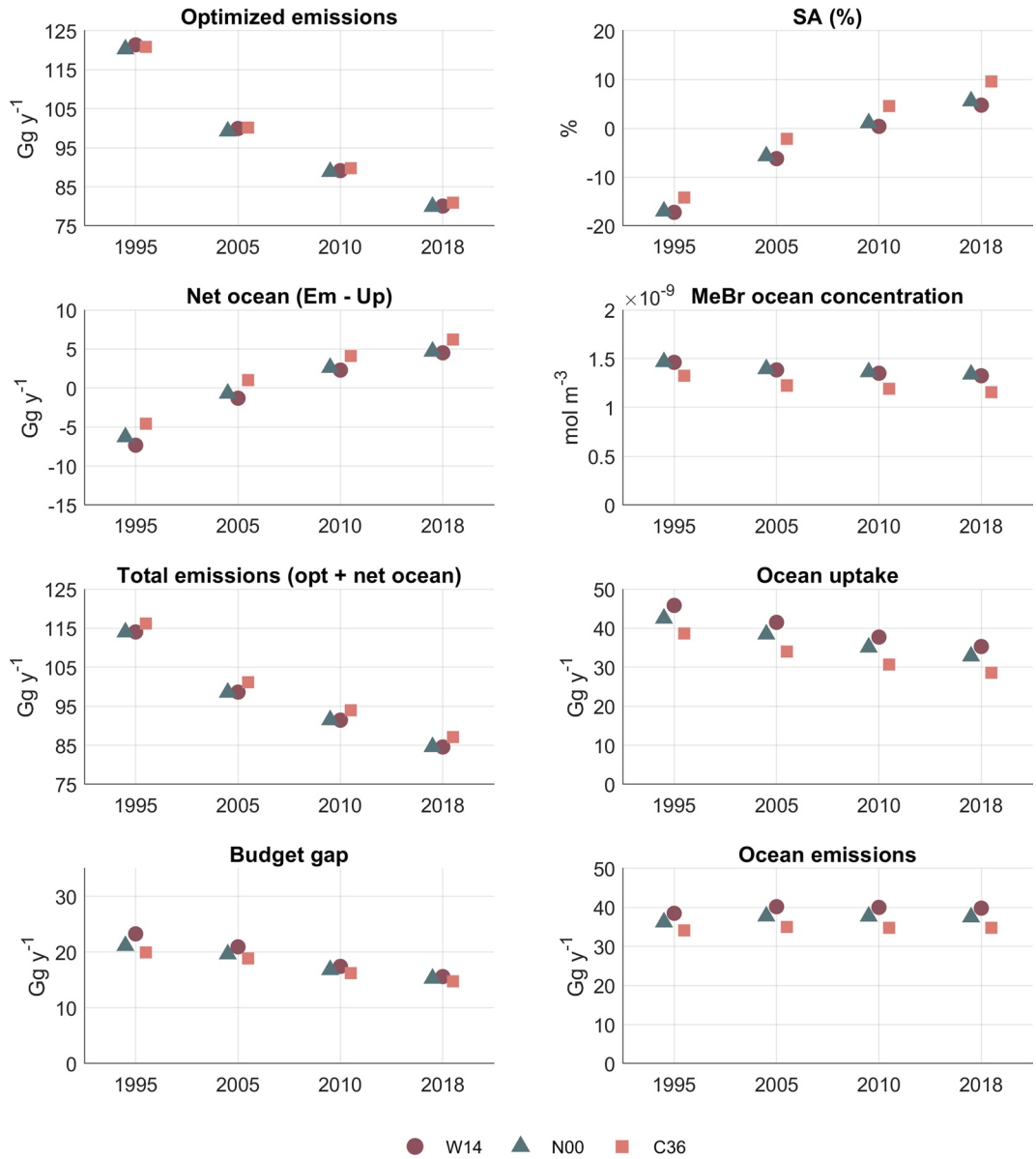

Figure 5. Methyl bromide global model inversion results from four time periods: pre phase-out (1995), 2005, 2010, and 2018. All quantities are global, area-weighted annual averages. Results are shown using three different gas transfer parameterizations with identical symbols and colors in all panels. Left side from top: 1) Optimized terrestrial emissions–emissions required to obtain agreement between model and National Oceanographic and Atmospheric Administration Global Monitoring Laboratory data set, 2) net ocean emissions (emissions–uptake; see text), 3) total emissions (terrestrial + net ocean), 4) budget gap–optimized terrestrial emissions minus the best estimate of known terrestrial sources. Right side from top: 1) globally averaged saturation anomaly, 2) methyl bromide surface ocean concentrations, 3) ocean uptake, and 4) ocean emissions.

gas transfer, rapid oceanic destruction), ocean methyl bromide levels are independent of atmospheric levels and ocean methyl bromide levels are less sensitive to externally imposed changes in atmospheric methyl bromide levels. This explains why the W14 parameterization with the largest k_{gas} and smallest R_o exhibits the largest changes in oceanic concentrations as phase-out progresses and atmospheric levels decline. Net ocean evasion for W14 changes from nearly −7.2 Gg y^{-1} prior to phase-out to +4.2 Gg y^{-1} after phase-out. By contrast, the COAREG 3.6 parameterization (smaller kgas, larger R) exhibits more symmetrical change in saturation state, from roughly −4.5 to +6.2 Gg y^{-1}.

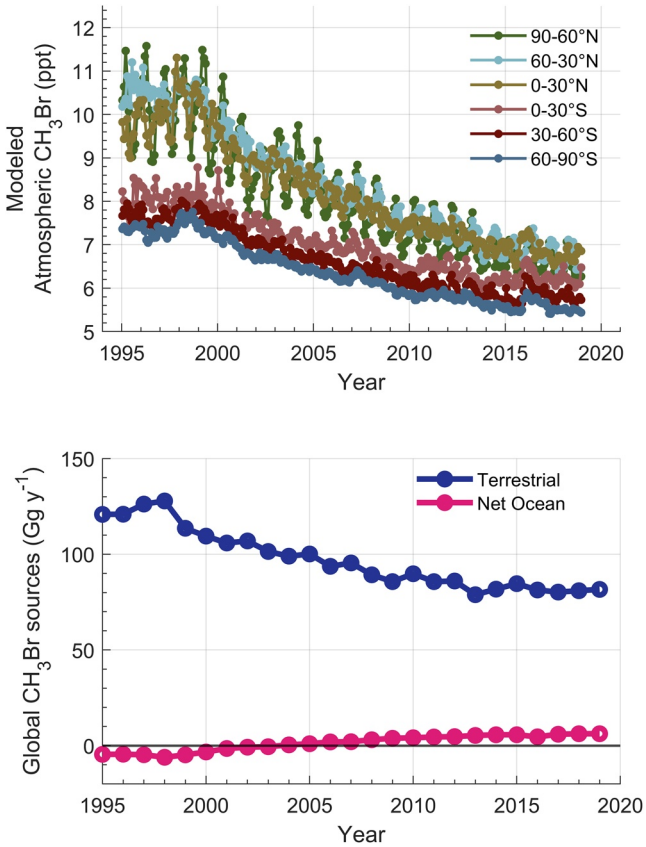

Figure 6. Results from global model inversion based on 1995–2019 National Oceanographic and Atmospheric Administration Global Monitoring Laboratory monthly observations using the COAREG 3.6 gas transfer parameterization. Upper panel: Model-generated tropospheric monthly methyl bromide mole fractions in the six zonal model boxes. Lower panel: Optimized total terrestrial emissions (blue), net ocean emissions (emissions–uptake; pink). Negative values for the ocean source from 1995 to 2000 indicate that the oceans were a net sink during that period.

4.2. Partitioning the Budget Gap Into Time-Dependent and Persistent Components

In this section, we examine the time dependence and latitudinal distribution of the methyl bromide budget gap using results from a model inversion of the full 1995–2019 record with the COAREG 3.6 gas transfer parameterization. As above, the budget gap is calculated as the difference between the bottom-up emission inventory and the total sources required by the model inversion. Figure 6

A bottom up *base case* inventory of terrestrial sources is defined based on the following:

Anthropogenic QPS, non-QPS, and leaded gasoline uses–QPS (quarantine and preshipment) and non-QPS emissions based on the UNEP national inventory reporting of methyl bromide consumption (production + import – export; ozone.unep.org). Emission factors of 0.84 and 0.65 are used to estimate emissions to the atmosphere from consumption data for QPS and non-QPS uses, respectively (Montzka & Reimann, 2011). Leaded gasoline emissions are based on Ozone Assessment Reports.

Biofuels——based on the magnitude, seasonal variability, and latitudinal distribution of biofuel burning in Yevich & Logan (2003), with updated methyl bromide emission factors from this type of burning given in Andreae (2019). Yearly changes are scaled to the biofuels and waste energy utilization history compiled by the International Energy Agency (IEA; www.iea.org/data).

Biomass burning—based on the Global Fire Emission Database (GFED4s) inventory of dry matter burned (van der Werf et al., 2017) as a function of year, month, and latitude with methyl bromide emission factors from Andreae (2019).

Vegetation emissions—fixed annual emissions of 28.5 Gg y^{-1} (Gan et al., 1998; Lee-Taylor & Holland, 2000; Rhew et al., 2000, 2001; Varner et al., 1999; Yvon-Lewis et al., 2009) scaled to latitudinal and seasonal variations of ISLSCP II, MODIS collection 4, IGPB Land Cover (Friedl et al., 2010).

Subtracting the sum of the bottom-up *base case* emissions from the total emissions required by the model to match the observations yields a missing source that declines from about 20 to 25 Gg y^{-1} during the late 1990s to 15–17 Gg y^{-1} in the 2015–2019 period (Figure 7). The decline in total emissions is clearly dominated by the temporal change in anthropogenic emissions, but partially offset by increasing net ocean emissions and the slight increase in biofuel emissions. On interannual time scales, there is also some evidence of anticorrelation between the missing source and biomass burning emissions, particularly around the 1997 and 2015 strong El Niño events. This perhaps suggests that burning emissions of methyl bromide may be underestimated in years following those major ENSO's.

The spatial distribution of the *base case* budget gap was obtained by subtracting the bottom-up emissions in each 30° zonal box from the total terrestrial emissions required by the model inversion in each box (Figure 7). A striking feature of the distribution is that the northern hemisphere mid-latitudes (30°–60°N) has a negative budget gap indicating the bottom-up, *base case* emissions were overestimated in that region. This signal is strongly anticorrelated with the positive budget gap in the adjacent northern hemisphere tropics/subtropic (0°–30°N). This could suggest that the bottom-up emissions were apportioned incorrectly between the two regions or that the very simple transport parameterization in the zonal model does an inadequate job of distributing agricultural emissions in the lower latitude regions of the midlatitude box such as California and Florida.

Based on UNEP methyl bromide consumption data, the agricultural non-QPS contribution to the methyl bromide budget after 2015 should be small and the uncertainty in this term should be negligible in comparison to the missing source. The budget gap (missing source) at this time is roughly 15 Gg y^{-1}. We assume these emissions

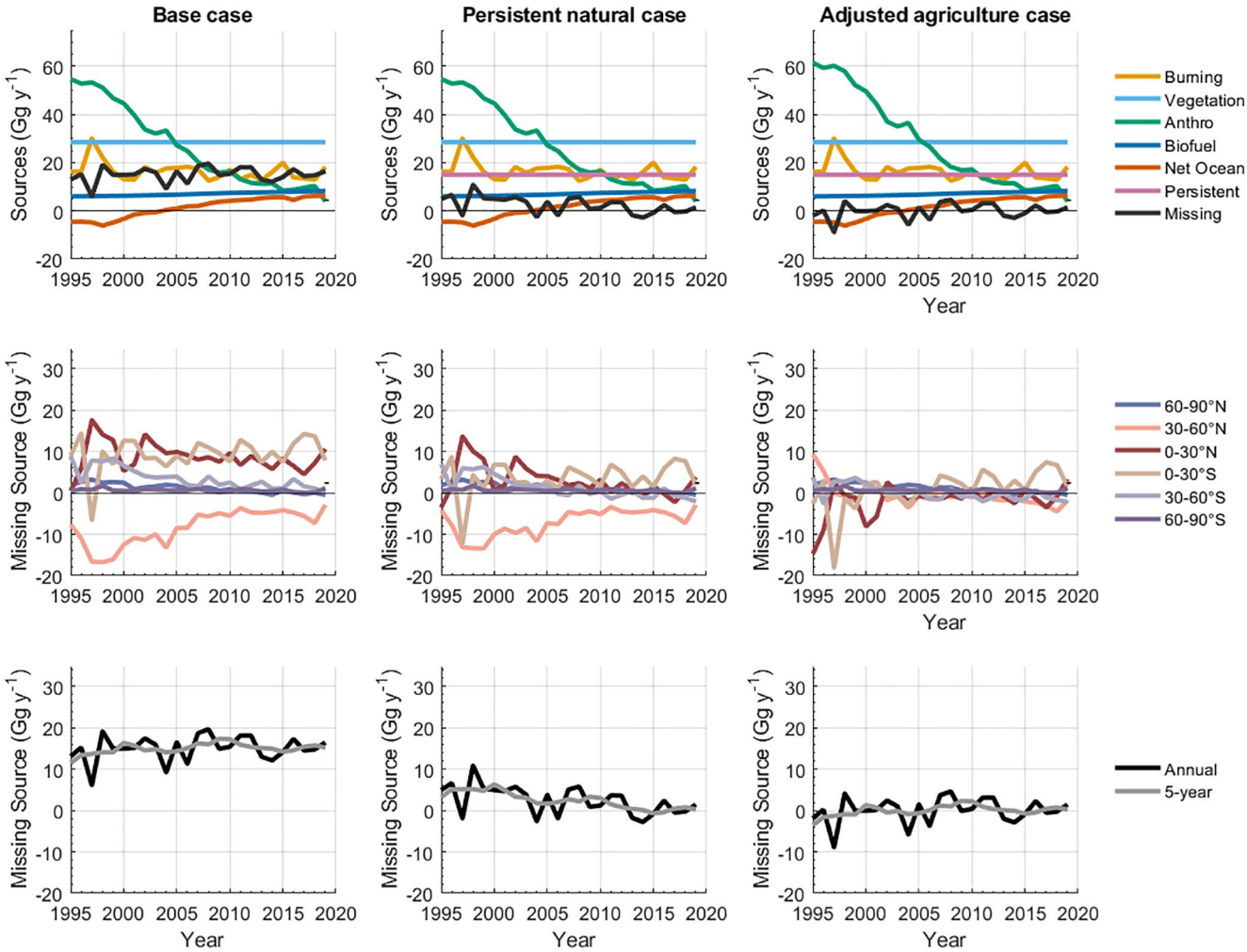

Figure 7. Results from the model inversion showing temporal and spatial characteristics of methyl bromide sources for three cases: *base case* (left column), *persistent natural case* (middle column), *and adjusted agriculture case* (right column). See text for description of cases. Top row: bottom-up inventory of global sources including the inferred budget gap (or missing source) based on the model inversion, middle row: latitudinal distribution of the budget gap, bottom row: budget gap between optimized emissions and estimated sources shown as annual mean (black) and 5-year running average (gray). See legends for color key.

must be comprised of one or more unknown or underestimated sources other than agricultural non-QPS sources. We call these *"persistent natural"* sources and provisionally assume that they have been present throughout the record. The latitudinal distribution of the missing source from 2015 to 2019 shows that it is predominantly in the tropics with a distribution similar to that of tropical vegetation emissions (45% in 0°–30°N, 40% in 0°–30°S, and 15% in 30°–60°S).

If we include a persistent tropical source of about 15 Gg y^{-1} during all years, the residual budget gap exhibits a time dependent decline from 15 to 20 Gg y^{-1} during the late 1990s to essentially zero from 2015 to 2019 (slope = −0.25 Gg y^{-1}, $p < 0.01$). The latitudinal distribution of the residual budget gap after subtraction of the persistent natural source is shown in Figure 7, and referred to as the *persistent natural case*. This decline is similar in timing to the scheduled phaseout of agricultural non-QPS use of methyl bromide. We therefore propose that the remaining, time-dependent part of the budget gap could reflect an underestimation of the agricultural non- QPS contribution.

The final scenario involves increasing the agricultural non-QPS source to reduce the magnitude of the time-dependent missing source and to reduce the anticorrelation between the northern midlatitudes and northern tropical regions (Figure 7). Two adjustments were made: (a) the fraction of methyl bromide that escapes to the atmosphere during agricultural fumigation was increased from 0.65 to 0.76, and (b) the spatial distribution of these emissions

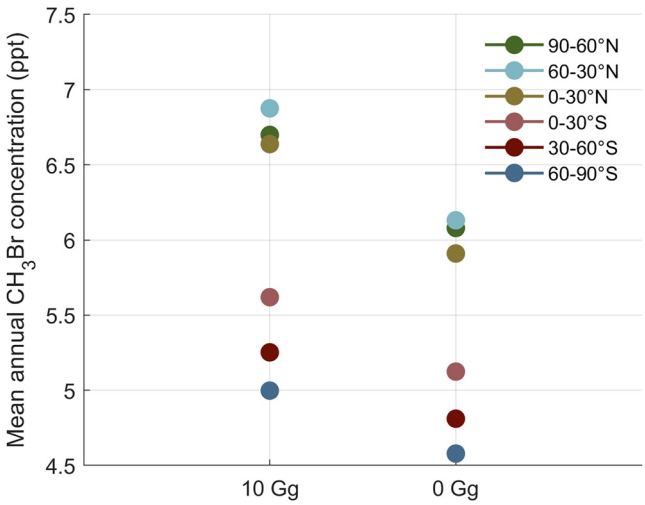

Figure 8. Atmospheric methyl bromide from model simulations based on 2018 budget with and without quarantine pre-shipments emissions. Data from simulations using the COAREG 3.6 gas transfer parameterization.

was shifted from a NH midlatitude:NH tropics ratio of 50:40 to 20:55. These adjustments to the fractional emission rate are within the uncertainty in bottom-up estimates for this source (Montzka & Riemann, 2011). The need to adjust the spatial distribution of the emissions are likely not due to reporting issues, but rather may be due to the overly simple transport parameterizations used in this box model. Simulations using a 3-D chemical transport model would be needed to fully understand why this geographic shift is required. This *adjusted agricultural* scenario has the expected effect of reducing the time-dependence of the missing source, reducing the apparent negative missing emissions in the northern midlatitudes, and reducing the overall magnitude of the missing source to 0.4 ± 3.1 Gg y^{-1} or essentially zero over the 1995–2019 period.

The proposed modifications to the methyl bromide budget alter the ratio of anthropogenic emissions to total emissions (optimized emissions + ocean emissions) compared to prior estimates (Figure S4 in Supporting Information S1). Anthropogenic emissions during 1996–1998 in the *base case* averaged 53 Gg yr^{-1}, or roughly 33% of total emissions. This is near the midpoint of the range of 22%–40% estimated for that period (Carpenter et al., 2014). With the *adjusted agricultural* scenario, the anthropogenic emissions comprise roughly 36% of total emissions for this period, near the upper end of the reported range.

4.3. A Simulation With Zero Anthropogenic Methyl Bromide Usage

As a final application of the model, atmospheric methyl bromide levels are simulated in a possible future scenario in which there is no intentional anthropogenic utilization of methyl bromide. This is done by conducting two forward model runs: (a) a *control case* using bottom-up emissions for 2018 (including the persistent natural source and adjusted agricultural sources), and (b) a *zero anthropogenic case* (with no emissions from agricultural, QPS, and leaded gasoline) with all other emissions as in the *control case* (Table S3 in Supporting Information S1). Biofuel, biomass burning, and terrestrial emissions were unchanged. The budgets and results from these simulations are summarized in the Supplemental Information (Table S3 in Supporting Information S1).

The *zero anthropogenic case* resulted in a reduction of the tropospheric methyl bromide burden by about 10% and a reduction in the total emissions (total terrestrial plus net ocean emissions) of about 9% relative to the 2018 *control case*. The N/S interhemispheric difference is 1.05 ppt in the *zero anthropogenic case*, reduced from 1.33 ppt in the *2018 control case*. The reductions in anthropogenic emissions are partially offset by the compensating effect of ocean/atmosphere exchange, which involves several coupled responses to the lowering of total terrestrial emissions. The main ocean response is decreased invasion and uptake, resulting from the decrease in atmospheric methyl bromide levels. Surface ocean concentrations change very little (less than 2%) because they are largely controlled by ocean production/loss (R_o = 0.83) so emissions and evasion remain nearly constant. As a result, there is a significant increase in the air/sea concentration difference and the area-weighted mean surface ocean supersaturation anomaly increases from 12.3% to 18.6%. The net effect of these changes is to increase the net air/sea exchange by 2.59 Gg yr^{-1}, offsetting some of the reduction in anthropogenic emissions.

The *zero anthropogenic* simulation generates an annual mean methyl bromide level of 4.6 ppt for the high latitude southern hemisphere and 4.9 ppt for the southern hemispheric mean (Figure 8). By comparison, Antarctic ice core measurements give a mean methyl bromide level of about 5.8 ppt for the late Holocene preindustrial (Saltzman et al., 2004, 2008). It is interesting the model estimate is below preindustrial, as the model includes modern biofuel and biomass burning emissions, which are generally believed to be elevated above late Holocene preindustrial values. There is also no basis for assuming that terrestrial vegetation or the persistant natural sources are constant. Such variability will likely determine future trends in atmospheric methyl bromide.

4.4. Assessing Uncertainties

Uncertainty in estimating the methyl bromide budget and budget gap reflects the propagated uncertainty in the atmospheric lifetime, terrestrial sources (vegetation, biomass burning, biofuels, and anthropogenic), and in oceanic methyl bromide production, cycling, and air/sea exchange. Uncertainties in transport coefficients or inadequacies in the parameterization of transport with a simple box model contribute to uncertainty in the spatial/temporal variability of the budget gap. A full discussion of uncertainties in the methyl bromide budget is beyond the scope of this paper, but many aspects have been discussed previously (Butler & Rodriguez, 1996; Montzka & Riemann, 2011; Yvon-Lewis et al., 2009). Here, we discuss a few of the uncertainties that were quantified during the course of this study.

The rate constant for methyl bromide reaction with OH has an estimated global weighted average uncertainty of about 9% (Burkholder et al., 2015). As a perturbation test, we reran the methyl bromide inversions for 1996 and 2019 with OH rate constants decreased by 10%. The methyl bromide emissions required to satisfy atmospheric observations were reduced by roughly 7 Gg y^{-1} in 1996 and 5 Gg y^{-1} in 2019 (Figure S5 in Supporting Information S1), with most of the reduction occurring in the tropics. The 10% reduction in OH rate constant results in a 6% reduction in total emissions (terrestrial plus net ocean) since OH is responsible for about half of the total atmospheric losses. This increase in atmospheric lifetime would not change our inference that the budget gap is comprised of both persistent and time-dependent sources. The reduction in OH loss would reduce the persistent missing source by about 30% (from 15 to 10 Gg y^{-1}) and slightly increase the agricultural adjustment (by about 2 Gg y^{-1} in 1996).

Stratospheric loss was parameterized in our simulations as a first order loss applied to all atmospheric boxes, rather than assigned predominantly to the tropics. Assigning the stratospheric loss to the tropics caused the optimized emissions in those regions to increase by about 1 Gg/yr (3%), with a corresponding decrease distributed across the other regions. The model also utilizes a very simple parameterization of atmospheric transport between the six atmospheric boxes. Varying the transport coefficients by 10% yielded a change of only 0.06 Gg y^{-1} in 1996 (0.3% of the missing source) and 0.08 Gg y^{-1} in 2019 (0.5% of the missing source). Such changes also alter the geographic/temporal assignment of the budget gap among the various boxes.

Uncertainty in the global budget due to gas transfer parameterization is estimated by comparing the differences between the three parameterizations. As shown in Figure 5, the differences in net ocean/atmosphere exchange between the various parameterizations ranged from 2 to 2.6 Gg/yr across the various years simulated. This represents only about 2% of total emissions in the various years. This uncertainty is small because the gas transfer parameterizations affect both ocean emissions and uptake, and only the net difference impacts the atmospheric budget. This is not the case when calculating atmospheric lifetimes, where only the uptake rate is important (Yvon-Lewis & Butler, 2002).

Temporal changes in sea surface temperature and winds occurred during the 1995–2019 time period. Nicewonger et al. (2022) showed that the effect of these changes on net ocean/atmosphere exchange (via solubility, hydrolysis, and gas transfer coefficient) were negligible. That study also examined the possible sensitivity of oceanic production to changes in sea surface temperature. The production rate used in this study (assumed constant) is observationally constrained by sea surface saturation anomaly measurements for the late 1990s and 2010 (Hu et al., 2012; King et al., 2002). Assuming the spatial relationship between methyl bromide production and sea surface temperature relationship also applies to temporal changes in temperature, they estimated that changes in sea surface temperature alone changed ocean production by less than 2%. This calculation does not account for possible changes in the biological state of the ocean resulting from changes in ocean circulation or nutrient distributions. Detecting such changes would require additional observational efforts to survey sea surface saturation state.

5. Conclusions

The NOAA GML flask air network provides a continuous global record of the changes in atmospheric methyl bromide prior to and during phase-out of anthropogenic emissions under the Montreal Protocol. The latest five years of this record are of particular interest because reported agricultural use has been fairly constant and has declined to a point where the uncertainty in those emissions are a very small fraction of the total terrestrial

emissions. The data suggest that the post phase-out atmospheric methyl bromide mole fraction has been roughly stable since 2015. As previously shown, the phase-out decline led to a continuous increase in ocean saturation state, shifting the oceans from a net sink to a net source. This model analysis shows that the differences between various parameterizations of gas transfer are a minor source of uncertainty in the global budget.

The use of updated gas transfer parameterizations and scatterometer-based ocean wind fields in this study results in total terrestrial methyl bromide emissions of about 128 Gg y^{-1} during the late 1990s at the peak of agricultural use. This is about 10% less than prior estimates using earlier gas transfer parameterizations, wind speed fields, and sea surface temperatures (Saltzman et al., 2004; Yvon-Lewis et al., 2009). The late 1990s "budget gap" is estimated at about 20 Gg y^{-1}, roughly 35% smaller than prior studies. For 2018, after atmospheric methyl bromide mole fraction stabilized post-phase-out, this study yields a budget gap of around 15 Gg y^{-1}, or 19% of the total terrestrial emissions.

The evolution of the budget gap before, during, and after phase-out provides some insight. The fact that a budget gap remains after phase-out suggests that unaccounted-for natural sources are important and likely persist throughout the 25 year observational record. Spatial analysis of this budget gap suggests it occurs primarily in the tropics and sub-tropics. The source may be related to terrestrial ecosystem emissions as previously speculated, but a specific source of sufficient magnitude remains to be identified.

The fact that the budget gap declines during phase-out as anthropogenic emissions decline, suggests that at least part of the gap results from underestimation of past anthropogenic emissions. We account for the time varying component of the budget gap by slightly increasing the estimated fraction of methyl bromide emitted during agricultural application and shifting the geographic location of agricultural emissions to be predominantly in the tropics for all years. We stress that the shifting of geographic location of agricultural emissions may be a non-physical artifact resulting from the highly simplified box model atmospheric transport. The proposed increase in past agricultural methyl bromide emissions from our analysis are within the estimated uncertainties associated with bottom-up estimates.

In summary, stabilization of post-phase-out atmospheric methyl bromide has provided an opportunity to revisit our understanding of the global methyl bromide cycle. Our results highlight the fact that even in a world with small anthropogenic emissions, significant uncertainties remain in the budget. Expanded observations to better detect meridional variability in atmospheric methyl bromide levels (particularly in the tropics) would provide improved constraints on major budget terms, and perhaps reveal the cause of the post-phase-out budget gap.

Data Availability Statement

Input data, model codes, and output data are publicly available through the Dryad (datadryad.org) and Zenodo (zenodo.org) repositories (Nicewonger and Saltzman, 2021). Input and output data are archived at https://doi.org/10.7280/D14979 and model code is archived at https://doi.org/10.5281/zenodo.4776409. The work is licensed under a CC0 1.0 Universal Public Domain Dedication license.

Acknowledgments
M. R. Nicewonger. was supported by National Research Council postdoctoral fellowship. We thank C. Siso for technical assistance in flask analysis, B. Hall for preparation and maintenance of gas standards, and station personnel at NOAA cooperative sampling locations for their assistance in collecting flask samples at remote sites across the globe. The measurements analyzed in this study were funded in part by the NOAA Climate Program Office's AC4 program.

References

Andreae, M. O. (2019). Emission of trace gases and aerosols from biomass burning–An updated assessment. *Atmospheric Chemistry and Physics*, *19*, 8523–8546. https://doi.org/10.5194/acp-19-8523-2019

Atlas, R., Hoffman, R. N., Ardizzone, J., Leidner, S. M., Jusem, J. C., Smith, D. K., & Gombos, D. (2011). A cross-calibrated, multiplatform ocean surface wind velocity product for meteorological and oceanographic applications. *Bulletin of the American Meteorological Society*, *92*(2), 157–174. https://doi.org/10.1175/2010BAMS2946.1

Burkholder, J. B., Sander, S. P., Abbatt, J., Barker, J. R., Huie, R. E., Kolb, C. E., et al. (2015). *Chemical kinetics and photochemical data for use in atmospheric studies evaluation no. 18 (JPL publication 15-10)*. Jet Propulsion Laboratory. Retrieved from https://jpldataeval.jpl.nasa.gov

Butler, J. H. (1994). The potential role of the ocean in regulating atmospheric CH_3BR. *Geophysical Research Letters*, *21*, 185–188. https://doi.org/10.1029/94GL00071

Butler, J. H., & Rodriguez, J. M. (1996). Methyl bromide in the atmosphere. In *The methyl bromide issue* (pp. 28–90). John Wiley & Sons Ltd.

Carpenter, L. J., Reimann, S., Engel, A., Burkholder, J. B., Clerbaux, C., Hall, B., et al. (2014). Ozone-depleting substances (ODSs) and other gases of interest to the Montreal Protocol. *Chapter 1 in Scientific Assessment of Ozone Depletion: 2014*. Global Ozone Research and Monitoring Project—Report. No. 55. World Meteorological Organization.

De Bruyn, W. J., & Saltzman, E. S. (1997a). Diffusivity of methyl bromide in water. *Marine Chemistry*, *57*(1–2), 55–59. https://doi.org/10.1016/S0304-4203(96)00092-8

De Bruyn, W. J., & Saltzman, E. S. (1997b). The solubility of methyl bromide in pure water, 35‰ sodium chloride and seawater. *Marine Chemistry*, *56*(1–2), 51–57. https://doi.org/10.1016/S0304-4203(96)00089-8

Deventer, M. J., Jiao, Y., Knox, S. H., Anderson, F., Ferner, M. C., Lewis, J. A., & Rhew, R. C. (2018). Ecosystem-scale measurements of methyl halide fluxes from a Brackish tidal marsh invaded with perennial pepperweed (lepidium latifolium). *Journal of Geophysical Research: Biogeosciences*, *123*(7), 2104–2120. https://doi.org/10.1029/2018JG004536

Engel, A., & Rigby, M. (2018). Update on ozone-depleting substances (ODSs) and other gases of interest to the Montreal Protocol. *Chapter 1 in Scientific Assessment of Ozone Depletion: 2018*, Global Ozone Research and Monitoring Project—Report. No. 58. World Meteorological Organization.

Fairall, C. W., Hare, J. E., Edson, J. B., & McGillis, W. (2000). Parameterization and micrometeorological measurement of air-sea gas transfer. *Boundary-Layer Meteorology*, *96*(1), 63–106. https://doi.org/10.1023/a:1002662826020

Fairall, C. W., Yang, M., Bariteau, L., Edson, J. B., Helmig, D., & McGillis, W. (2011). Implementation of the coupled ocean-atmosphere response experiment flux algorithm with CO_2, dimethyl sulfide, and O_3. *Journal of Geophysical Research*, *116*, C00F09. https://doi.org/10.1029/2010JC006884

Friedl, M. A., Strahler, A. H., Hodges, J., Hall, F. G., Collatz, G. J., Meeson, B. W., et al. (2010). *ISLSCP II MODIS (collection 4) IGBP land cover, 2000-2001*. ORNL DAAC. https://doi.org/10.3334/ORNLDAAC/968

Gan, J., Yates, S. R., Ohr, H. D., & Sims, J. J. (1998). Production of methyl bromide by terrestrial higher plants. *Geophysical Research Letters*, *25*(19), 3595–3598. https://doi.org/10.1029/98gl52697

Hardacre, C. J., & Heal, M. R. (2013). Characterization of methyl bromide and methyl chloride fluxes at temperate freshwater wetlands. *Journal of Geophysical Research: Atmospheres*, *118*(2), 977–991. https://doi.org/10.1029/2012JD018424

Ho, D. T., Wanninkhof, R., Schlosser, P., Ullman, D. S., Hebert, D., & Sullivan, K. F. (2011). Toward a universal relationship between wind speed and gas exchange: Gas transfer velocities measured with $^3He/SF_6$ during the Southern Ocean Gas Exchange Experiment. *Journal of Geophysical Research*, *116*(7), 1–13. https://doi.org/10.1029/2010JC006854

Hu, L., Yvon-Lewis, S., Liu, Y., & Bianchi, T. S. (2012). The ocean in near equilibrium with atmospheric methyl bromide. *Global Biogeochemical Cycles*, *26*(3), 1–11. https://doi.org/10.1029/2011GB004272

Jiao, Y., Acdan, J., Xu, R., Deventer, M. J., Zhang, W., & Rhew, R. C. (2020). Global methyl halide emissions from rapeseed (Brassica napus) using life cycle measurements. *Geophysical Research Letters*, *47*(19), 1–9. https://doi.org/10.1029/2020GL089373

King, D. B., Butler, J. H., Yvon-Lewis, S. A., & Cotton, S. A. (2002). Predicting oceanic methyl bromide saturation from SST. *Geophysical Research Letters*, *29*(24), 2–5. https://doi.org/10.1029/2002GL016091

Lee-Taylor, J. M., Doney, S. C., Brasseur, G. P., & Muller, J.-F. (1998). A global three-dimensional atmosphere-ocean model of methyl bromide distributions. *Journal of Geophysical Research*, *103*, 16039–16057. https://doi.org/10.1029/98JD00970

Lee-Taylor, J. M., & Holland, E. A. (2000). Litter decomposition as a potential natural source of methyl bromide. *Journal of Geophysical Research*, *105*(D7), 8857–8864. https://doi.org/10.1029/1999JD901112

Marik, T. (1998). *Atmospheric $\delta^{13}C$ and δD measurements to balance the global methane budget* (PhD thesis). Ruprecht-Karls-University.

McGillis, W. R., Dacey, J. W. H., Frew, N. M., Bock, E. J., & Nelson, R. K. (2000). Water-air flux of dimethylsulfide. *Journal of Geophysical Research*, *105*(C1), 1187–1193. https://doi.org/10.1029/1999JC900243

Mitchell, L., Brook, E., Lee, J. E., Buizert, C., & Sowers, T. (2013). Constraints on the late holocene anthropogenic contribution to the atmospheric methane budget. *Science*, *342*(6161), 964–966. https://doi.org/10.1126/science.1238920

Montzka, S. A., Butler, J. H., Hall, B. D., Mondeel, D. J., & Elkins, J. W. (2003). A decline in tropospheric organic bromine. *Geophysical Research Letters*, *30*(15), 1–4. https://doi.org/10.1029/2003GL017745

Montzka, S. A., & Reimann, S. (2011). Ozone depleting substances (ODSs) and related chemicals. *Chapter 1 in Scientific Assessment of Ozone Depletion: 2010*, Global Ozone Research and Monitoring Project—Report. No. 52. World Meteorological Organization.

Naegler, T. (2009). Reconciliation of excess ^{14}C-constrained global CO_2 piston velocity estimates. *Tellus, Series B: Chemical and Physical Meteorology*, *61*(2), 372–384. https://doi.org/10.1111/j.1600-0889.2008.00408.x

Naegler, T., & Levin, I. (2006). Closing the global radiocarbon budget 1945-2005. *Journal of Geophysical Research*, *111*(D12), 1–14. https://doi.org/10.1029/2005JD006758

Nicewonger, M., & Saltzman, E. S. (2021). *Methyl bromide atmosphere-ocean box model code, inputs, and outputs*. https://doi.org/10.7280/D14979

Nicewonger, M. R., Saltzman, E. S., & Montzka, S. A. (2022). ENSO-driven fires cause large interannual variability in the naturally emitted, ozone-depleting trace gas CH_3Br. *Geophysical Research Letters*, *49*, e2021GL094756. https://doi.org/10.1029/2021GL094756

Nightingale, P. D., Malin, G., Law, C. S., Watson, A. J., Liss, P. S., Liddicoat, M. I., et al. (2000). In situ evaluation of air-sea gas exchange parameterizations using novel conservative and volatile tracers. *Global Biogeochemical Cycles*, *14*(1), 373–387. https://doi.org/10.1029/1999GB900091

Orkin, V. L., Khamaganov, V. G., Kasimovskaya, E. E., & Guschin, A. G. (2013). Photochemical properties of some Cl-containing halogenated alkanes. *The Journal of Physical Chemistry A*, *117*, 5483–5490. https://doi.org/10.1021/jp400408y

Prather, M. J., Holmes, C. D., & Hsu, J. (2012). Reactive greenhouse gas scenarios: Systematic exploration of uncertainties and the role of atmospheric chemistry. *Geophysical Research Letters*, *39*(9), 6–10. https://doi.org/10.1029/2012GL051440

Reynolds, R. W., Rayner, N. A., Smith, T. M., Stokes, D. C., & Wang, W. (2002). An improved in situ and satellite SST analysis for climate. *Journal of Climate*, *15*(13), 1609–1625. https://doi.org/10.1175/1520-0442(2002)015<1609:aiisas>2.0.co;2

Rhew, R. C., Chen, C., Teh, Y. A., & Baldocchi, D. (2010). Gross fluxes of methyl chloride and methyl bromide in a California oak-Savanna woodland. *Atmospheric Environment*, *44*(16), 2054–2061. https://doi.org/10.1016/j.atmosenv.2009.12.014

Rhew, R. C., Miller, B. R., Vollmer, M. K., & Weiss, R. F. (2001). Shrubland fluxes of methyl bromide and methyl chloride. *Journal of Geophysical Research*, *106*(D18), 20875–20882. https://doi.org/10.1029/2001JD000413

Rhew, R. C., Miller, B. R., & Weiss, R. F. (2000). Natural methyl bromide and methyl chloride emissions from coastal salt marshes. *Nature*, *403*, 292–295. https://doi.org/10.1038/35002043

Saltzman, E. S., Aydin, M., De Bruyn, W. J., King, D. B., & Yvon-Lewis, S. A. (2004). Methyl bromide in preindustrial air: Measurements from an Antarctic ice core. *Journal of Geophysical Research*, *109*, 1–8. https://doi.org/10.1029/2003jd004157

Saltzman, E. S., Aydin, M., Tatum, C., & Williams, M. B. (2008). A 2,000-year record of atmospheric methyl bromide from a South Pole ice core. *Journal of Geophysical Research*, *113*, D05304. https://doi.org/10.1029/2007JD008919

Shorter, J. H., Kolb, C. E., Crill, P. M., Kerwin, R. A., Talbot, R. W., Hines, M. E., & Harriss, R. C. (1995). Rapid degradation of atmospheric methyl bromide in soils. *Nature*, *377*(6551), 717–719. https://doi.org/10.1038/377717a0

Smith, W. H. F., & Sandwell, D. T. (1997). Global sea floor topography from satellite altimetry and ship depth soundings. *Science*, *277*(5334), 1956–1962. https://doi.org/10.1126/science.277.5334.1956

Spivakovsky, C. M., Logan, J. A., Montzka, S. A., Balkanski, Y. J., Jones, D. B. A., Horowitz, L. W., et al. (2000). Three-dimensional climatological distribution of tropospheric OH: Update and evaluation. *Journal of Geophysical Research*, *105*(D7), 8931–8980. https://doi.org/10.1029/1999JD901006

Sweeney, C., Gloor, E., Jacobson, A. R., Key, R. M., McKinley, G., Sarmiento, J. L., & Wanninkhof, R. (2007). Constraining global air-sea gas exchange for CO_2 with recent bomb ^{14}C measurements. *Global Biogeochemical Cycles*, *21*(2), 1–10. https://doi.org/10.1029/2006GB002784

UNEP (United Nations Environment Programme). (2014). In M. Pizano, I. Porter, & M. Besri (Eds.), *2014 Report of the Methyl Bromide Technical Options Committee*.

UNEP (United Nations Environment Programme). (2019). *Ozone secretariat country data center*. Retrieved from https://ozone.unep.org/countries/data

van der Werf, G. R., Randerson, J. T., Giglio, L., van Leeuwen, T. T., Chen, Y., Rogers, B. M., et al. (2017). Global fire emissions estimates during 1997-2016. *Earth System Science Data*, *9*(2), 697–720. https://doi.org/10.5194/essd-9-697-2017

Varner, R. K., Crill, P. M., & Talbot, R. W. (1999). Wetlands: A potentially significant source of atmospheric methyl bromide and methyl chloride. *Geophysical Research Letters*, *26*(16), 2433–2436. https://doi.org/10.1029/1999gl900587

Wanninkhof, R. (1992). Relationship between wind speed and gas exchange over the ocean. *Journal of Geophysical Research*, *97*(C5), 7373–7382. https://doi.org/10.1029/92JC00188

Wanninkhof, R. (2014). Relationship between wind speed and gas exchange over the ocean revisited. *Limnology and Oceanography: Methods*, *12*(6), 351–362. https://doi.org/10.4319/lom.2014.12.351

Wanninkhof, R., Asher, W. E., Ho, D. T., Sweeney, C., & McGillis, W. R. (2009). Advances in quantifying air-sea gas exchange and environmental forcing. *Annual Review of Marine Science*, *1*, 213–244. https://doi.org/10.1146/annurev.marine.010908.163742

Wentz, F. J., Scott, J., Hoffman, R., Leidner, M., Atlas, R., & Ardizzone, J. (2015). Remote sensing systems cross-calibrated multi-platform (CCMP) 6-hourly ocean vector wind analysis product on 0.25 deg grid, Version 2.0. Remote Sensing Systems. (Accessed 01 Feb 2021). Retrieved from www.remss.com/measurements/ccmp

Woolf, D. (1997). Bubbles and their role in gas exchange. In P. Liss, & R. Duce (Eds.), *The Sea surface and global change* (pp. 173–206). Cambridge University Press. https://doi.org/10.1017/CBO9780511525025.007

Yevich, R., & Logan, J. A. (2003). An assessment of biofuel use and burning of agricultural waste in the developing world. *Global Biogeochemical Cycles*, *17*(4), 1095. https://doi.org/10.1029/2002GB001952

Yvon-Lewis, S. A., & Butler, J. H. (1996). An improved estimate of the oceanic lifetime of atmospheric CH_3Br. *Geophysical Research Letters*, *23*(1), 53–56. https://doi.org/10.1029/95GL03022

Yvon-Lewis, S. A., & Butler, J. H. (1997). The potential effect of oceanic biological degradation on the lifetime of atmospheric CH_3Br. *Geophysical Research Letters*, *24*(10), 1227–1230. https://doi.org/10.1029/97GL01090

Yvon-Lewis, S. A., & Butler, J. H. (2002). Effect of oceanic uptake on atmospheric lifetimes of selected trace gases. *Journal of Geophysical Research*, *107*(D20), 4414. https://doi.org/10.1029/2001JD001267

Yvon-Lewis, S. A., Saltzman, E. S., & Montzka, S. A. (2009). Recent trends in atmospheric methyl bromide: Analysis of post-Montreal Protocol variability. *Atmospheric Chemistry and Physics*, *9*(16), 5963–5974. https://doi.org/10.5194/acp-9-5963-2009

Reference From the Supporting Information

Li, Y. H., Peng, T. H., Broecker, W. S., & Östlund, H. G. (1984). The average vertical mixing coefficient for the oceanic thermocline. *Tellus B: Chemical and Physical Meteorology*, *36*(3), 212–217. https://doi.org/10.3402/tellusb.v36i3.14905